RAA 2014 Vol. **14** No. **8**, 971–978 doi: 10.1088/1674–4527/14/8/007
http://www.raa-journal.org *http://www.iop.org/journals/raa*

***R**esearch in*
***A**stronomy and*
***A**strophysics*

Neutrino energy spectrum and electron capture of Nuclides ^{56}Fe, ^{56}Co, ^{56}Ni, ^{56}Mn, ^{56}Cr and ^{56}V in stellar interiors

Jing-Jing Liu

College of Science and Technology, Qiongzhou University, Sanya 572022, China;
liujingjing68@126.com

Received 2013 April 21; accepted 2013 October 8

Abstract Based on the shell-model Monte Carlo method and random phase approximation theory, the neutrino energy spectrum (NES) and the electron capture (EC) of ^{56}Fe, ^{56}Co, ^{56}Ni, ^{56}Mn, ^{56}Cr and ^{56}V are investigated in presupernova surroundings. The results show that the EC rates are affected greatly at different densities and temperatures. The rates increase greatly and even exceed six orders of magnitude at lower temperature. On the other hand, the NES is very sensitive to stellar temperature and electron energy. The higher the temperature and the lower the electron energy, the larger the influence on NES is. For example, the maxima of NES in the ground state are 9.02, 160, 80, 24.01, 0.44, 1.42 $m_{\rm e}\,c^2$ for ^{56}Fe, ^{56}Co, ^{56}Ni, ^{56}Mn, ^{56}Cr and ^{56}V respectively at $\rho_7 = 10.7, Y_{\rm e} = 0.45$ and $T_9 = 15$. Furthermore, the influence on NES due to EC for different nuclei has some otherness because of different Q_0-values. For example, the spectrum of ^{56}Co shows a double bump structure.

Key words: physical data and processes: neutrinos, nuclear reactions — stars: supernovae — stars: evolution

1 INTRODUCTION

The emission, scattering and energy loss of neutrinos have great importance in astrophysics. The neutrino energy loss (NEL) due to electron capture (EC) plays an important role in the process of supernova explosions. The neutrinos not only transport an enormous amount of energy outward, but also carry a lot of information about their stellar interiors. Thus, it is very important to investigate the NEL and the neutrino energy spectrum (hereafter NES) that occur in EC reactions, especially for some iron group nuclei.

Weak interactions (e.g. EC and beta decay) play a central role in the final evolution of massive stars. The EC rates of nuclides ^{56}Fe, ^{56}Co, ^{56}Ni, ^{56}Mn, ^{56}Cr and ^{56}V are a very important and dominant factor during the process of supernova explosions. Pioneering works on EC rates were investigated by some authors (Aufderheide et al. 1990, 1994; Langanke & Martinez-Pinedo 1998; Liu 2012, 2013a,b,c,d,e,f; Fuller et al. 1982) under the conditions of a supernova-like explosion. Liu & Luo (2007a,b); Liu et al. (2007a,b); Liu & Luo (2008a,b,c); Liu (2010a,b); Liu et al. (2011) also discussed the NEL and weak interactions of some iron group nuclides in presupernova conditions.

Due to the importance of nuclides ^{56}Fe, ^{56}Co, ^{56}Ni, ^{56}Mn, ^{56}Cr and ^{56}V in astrophysical surroundings, in this paper we focus on these nuclides and investigate their NES due to EC according to the shell-model Monte Carlo (SMMC) method, which has been discussed at length by Dean et al.

(1998). We also discuss the electron-capture cross section (ECCS) with the theory of random phase approximation (hereafter RPA). This paper is organized as follows: in the next section, we analyze the NES due to the EC process that occurs in stellar interiors. In Section 3 we discuss the effect of NES in ^{56}Fe, ^{56}Co, ^{56}Ni, ^{56}Mn, ^{56}Cr and ^{56}V. Some conclusions are given in Section 4.

2 THE NEUTRINO ENERGY SPECTRUM DUE TO EC IN STELLAR INTERIORS

The stellar EC rates for the k-th nucleus (Z, A) in thermal equilibrium at temperature T are given by a sum over the initial parent states i and the final daughter states f (Fuller et al. 1982)

$$\lambda_k = \lambda_{\rm ec} = \sum \frac{(2J_i+1)\mathrm{e}^{\frac{-E_i}{kT}}}{G(Z,A,T)} \sum_f \lambda_{if}, \tag{1}$$

where J_i and E_i are the spin and excitation energies of the parent states and the EC rates from one of the initial states to all possible final states are λ_{if}. $G(Z, A, T)$ is the nuclear partition function which is given by

$$G(Z,A,T) = \sum_i (2J_i+1) \exp\Big(-\frac{E_i}{kT}\Big). \tag{2}$$

According to the level density formula, when the contribution from the excited states is discussed, the nuclear partition function approximately becomes (Aufderheide et al. 1994)

$$\begin{aligned} G(Z,A,T) \ \approx\ & (2J_0+1) + \int_0^\infty dE \int_{J,\pi} dJ d\pi (2J_i+1) \\ & \times \vartheta(E,J,\pi) \exp\Big(-\frac{E_i}{kT}\Big), \end{aligned} \tag{3}$$

where the level density is given by (Holmes et al. 1976; Thielemann et al. 1986)

$$\vartheta(E,J,\pi) = \frac{1}{\sqrt{2\pi}\sigma} \frac{\sqrt{\pi}}{12a^{\frac{1}{4}}} \times \frac{\exp[2\sqrt{a(E-\delta)}]}{(E-\delta)^{\frac{5}{4}}} \zeta(E,J,\pi), \tag{4}$$

with

$$\zeta(E,J,\pi) = \frac{1}{2} \frac{(2J+1)}{2\sigma^2} \exp\Big[-\frac{J(J+1)}{2\sigma^2}\Big], \tag{5}$$

where a is the level density parameter and δ is the backshift (pairing correction). σ is defined as

$$\sigma = \Big(\frac{2m_u AR^2}{2\hbar^2}\Big)^{\frac{1}{2}} \Big[\frac{(E-\delta)}{a}\Big]^{\frac{1}{4}}, \tag{6}$$

where R is the radius and $m_u = \frac{1}{N_A}$ is the atomic mass unit.

Based on the theory of RPA (Dean et al. 1998) with a global parameterization of the single particle numbers, the EC rates are related to ECCS $\sigma_{\rm ec}$ by (Juodagalvis et al. 2010)

$$\lambda_{if} = \frac{1}{\pi^2\hbar^3} \sum_{if} \int_{\varepsilon_0}^\infty p_{\rm e}^2 \sigma_{\rm ec}(\sigma_n, \sigma_i, \sigma_f) f(\sigma_n, U_F, T) d\varepsilon_n, \tag{7}$$

where $\varepsilon_0 = \max(Q_{if}, 1)$. $p_{\rm e} = \sqrt{\varepsilon_n - 1}$ is the momentum of the incoming electron with energy ε_n, U_F is the electron chemical potential and T is the electron temperature. Note that in this paper all of the energies and momenta are respectively expressed in units of $m_{\rm e}c^2$ and $m_{\rm e}c$, where $m_{\rm e}$ is the electron mass and c is the speed of light.

The electron chemical potential is found by inverting the expression for the lepton number density

$$n_{\rm e} = \frac{\rho}{\mu_{\rm e}} = \frac{8\pi}{(2\pi)^3}\int_0^\infty p_{\rm e}^2(f_{-\rm e} - f_{+\rm e})dp_{\rm e}, \tag{8}$$

where ρ is the density in $\rm g\ cm^{-3}$ and $\mu_{\rm e}$ is the average molecular weight. $\lambda_{\rm e} = \frac{h}{m_{\rm e}c}$ is the Compton wavelength, $f_{-\rm e} = \left[1+\exp\left(\frac{\varepsilon_n - U_F - 1}{kT}\right)\right]^{-1}$ and $f_{+\rm e} = \left[1+\exp\left(\frac{\varepsilon_n + U_F + 1}{kT}\right)\right]^{-1}$ are the electron and positron distribution functions respectively and k is the Boltzmann constant.

The NES for a specific nuclear transition from i to f is given by the respective partial rate per energy interval. The total spectrum is then the sum over all possible transitions. The normalized neutrino spectrum is $N^{\nu}(\varepsilon_{\nu})$, which is obtained by dividing by the total electron capture rate. Based on the calculation of the partial cross section, the NES of the emitted neutrinos due to EC reactions is given by (Langanke & Martinez-Pinedo 1998)

$$N^{\nu}(\varepsilon_{\nu}) = \frac{1}{\lambda_{\rm ec}}\frac{1}{\pi^2\hbar^3}\sum_{if} p_{\rm e}^2\sigma_{\rm ec}(\varepsilon_n, \varepsilon_i, \varepsilon_f) f(\varepsilon_n, U_F, T), \tag{9}$$

where $\varepsilon_{\rm e} = \varepsilon_i - \varepsilon_f + \varepsilon_{\nu}$ and $p_{\rm e}$ is the corresponding momentum of the electron. The phase space factor is defined as

$$f(\varepsilon_n, U_F, T) = \left[1 + \exp\left(\frac{\varepsilon_n - U_F}{kT}\right)\right]^{-1}, \tag{10}$$

for an electron with energy ε_n from an initial proton in the single particle state with energy ε_i to a neutron in the single particle state with energy ε_f. Due to energy conservation, the electron, proton and neutron energies are related to the neutrino energy and Q –value for the capture reaction (Cooperstein & Wambach 1984)

$$Q_{i,f} = \varepsilon_{\rm e} - \varepsilon\nu = \varepsilon_n - \varepsilon_{\nu} = \varepsilon_f^n - \varepsilon_i^p\,, \tag{11}$$

so we have

$$\varepsilon_f^n - \varepsilon_i^p = \varepsilon_{if}^* + \hat{\mu} + \Delta_{\rm np}, \tag{12}$$

where $\hat{\mu} = \mu_{\rm n} - \mu_{\rm p}$, is the difference between the chemical potentials of the neutron and proton in the nucleus and $\Delta_{\rm np} = M_{\rm n}c^2 - M_{\rm p}c^2 = 1.293\ \rm MeV$ is the mass difference between the neutron and the proton. $Q_{00} = M_f c^2 - M_i c^2 = \hat{\mu} + \Delta_{\rm np}$, with M_i and M_f being the masses of the parent nucleus and the daughter nucleus respectively; ε_{if}^* corresponds to the excitation energies in the daughter nucleus at the states with zero temperature.

The total cross section for EC is (Dean et al. 1998)

$$\begin{aligned}\sigma_{\rm ec} = \sigma_{\rm ec}(\varepsilon_n) &= \sum_{if}\frac{(2J_i+1)\exp(-\beta E_i)}{Z_A}\sigma_{fi}(Ee) \\ &= \sum_{if}\frac{(2J_i+1)\exp(-\beta E_i)}{Z_A}\sigma_{fi}(En) \\ &= 6g_{\rm wk}^2\int d\xi(\varepsilon_n - \xi)^2\frac{G_A^2}{12\pi}S_{\rm GT+}(\xi)F(Z, \varepsilon_n),\end{aligned} \tag{13}$$

where $g_{\rm wk} = 1.1661\times10^{-5}\ \rm GeV^{-2}$ is the weak coupling constant and G_A is the axial vector's form-factor which at zero momentum is $G_A = 1.25$. The ε_n is the sum of the total rest mass and kinetic energies; $F(Z, \varepsilon_n)$ is the Coulomb wave correction which is the ratio of the square of the electron wave function distorted by the Coulomb scattering potential to the square of the wave function of the free electron.

$S_{\mathrm{GT}+}$ is the total amount of Gamow-Teller (GT) strength available for an initial state, which is given by summing over a complete set of final states in the GT transition matrix elements $|M_{\mathrm{GT}}|^2_{if}$. The SMMC method is also used to calculate the response function $R_A(\tau)$ of an operator $\hat{A}$ at an imaginary time τ, by using a spectral distribution of initial and final states $|i\rangle$ and $|f\rangle$ with energies E_i and E_f respectively. $R_A(\tau)$ is given by (Langanke & Martinez-Pinedo 1998)

$$R_A(\tau) = \frac{\sum_{if}(2J_i+1)\mathrm{e}^{-\beta E_i}\mathrm{e}^{-\tau(E_f-E_i)}|\langle f|\hat{A}|i\rangle|^2}{\sum_i(2J_i+1)\mathrm{e}^{-\beta E_i}}. \tag{14}$$

Note that the total strength for the operator is given by $R(\tau = 0)$. The strength distribution is given by

$$\begin{aligned} S_{\mathrm{GT}^+}(E) &= \frac{\sum_{if}\delta(E-E_f+E_i)(2J_i+1)\mathrm{e}^{-\beta E_i}|\langle f|\hat{A}|i\rangle|^2}{\sum_i(2J_i+1)\mathrm{e}^{-\beta E_i}} \\ &= S_A(E), \end{aligned} \tag{15}$$

which is related to $R_A(\tau)$ by a Laplace Transform, $R_A(\tau) = \int_{-\infty}^{\infty} S_A(E)\mathrm{e}^{-\tau E}dE$. Note that here E is the energy transfer within the parent nucleus, and that the strength distribution $S_{\mathrm{GT}^+}(E)$ has units of MeV^{-1} and $\beta = \frac{1}{T_{\mathrm{N}}}$, where T_{N} is the nuclear temperature.

The EC rates are given by integrating the total cross section with the flux of a degenerate relativistic electron gas

$$\lambda_{\mathrm{ec}} = \frac{\ln 2}{6163}\int_0^{\infty} d\xi S_{\mathrm{GT}} \frac{c^3}{(m_{\mathrm{e}}\, c^2)^5}\int_{p_0}^{\infty} dp_{\mathrm{e}} p_{\mathrm{e}}^2(-\xi+\varepsilon_n)^2 F(Z,\varepsilon_n) f(\varepsilon_n, U_F, T)\,. \tag{16}$$

The p_0 is defined as

$$p_0 = \begin{cases} \sqrt{Q_{if}^2 - 1} & (Q_{if} < -1) \\ 0 & (\mathrm{otherwise})\,. \end{cases} \tag{17}$$

3 THE STUDY AND DISCUSSION OF EC RATES AND NES

Figures 1 and 2 show the EC rates of ^{56}Fe, ^{56}Co, ^{56}Ni, ^{56}Mn, ^{56}Cr and ^{56}V as a function of T_9 at different astronomical conditions (ρ_7 is the density in units of $10^7\mathrm{g\ cm}^{-3}$ and T_9 is the temperature in units of 10^9 K). One can see the EC rates are affected greatly at different densities and temperatures. The rates increase greatly and even exceed six orders of magnitude at lower temperature. The lower the temperature, the larger the influence on EC is, because the electron energy is so low at lower temperatures that the EC rates can be strongly affected. On the other hand, owing to the fact that the electron energy is so high at higher temperatures, the higher the density, the smaller the influence on EC becomes. With an increase of the density, there are different effects on EC for different nuclides. This is caused by different Q-values and the orbital transitions. The Q-values of nuclides ^{56}Fe, ^{56}Mn, ^{56}Cr and ^{56}V are negative, but those for the others are positive (e.g. $Q_0 = 4.06$ MeV and 1.62 MeV for ^{56}Co and ^{56}Ni, respectively).

Figures 3, 4 and 5 show the NES of ^{56}Fe, ^{56}Co, ^{56}Ni, ^{56}Mn, ^{56}Cr and ^{56}V as a function of neutrino energy at $\rho_7 = 5.86$ and $Y_{\mathrm{e}} = 0.47$ and temperature of $T_9 = 7, 9, 11, 13$ and 15. One can see the neutrino energy has different effects on NES at the same density and different temperatures. The higher the temperature, the larger the influence on NES is. The higher the temperature, the higher the peak value of the NES is, because the electron energy is so large at relatively higher temperatures that the EC rates are strongly affected. This would lead to more and more electrons being affected

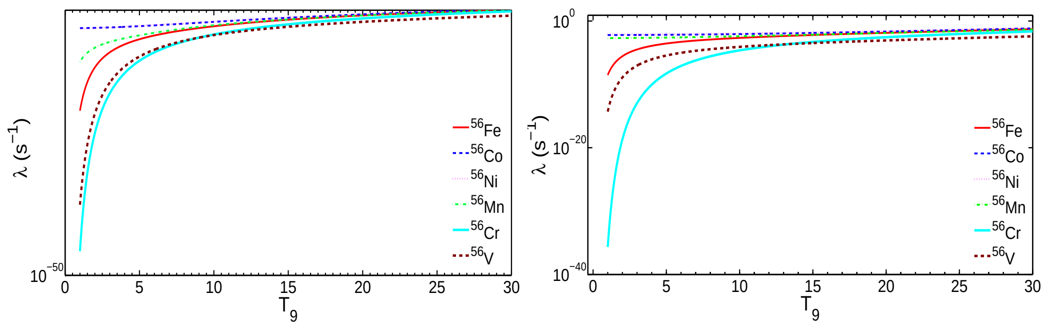

Fig. 1 The EC rates as a function of T_9 at the density $\rho_7 = 0.443, Y_\mathrm{e} = 0.48$ (*left*) and $\rho_7 = 14.5, Y_\mathrm{e} = 0.45$ (*right*).

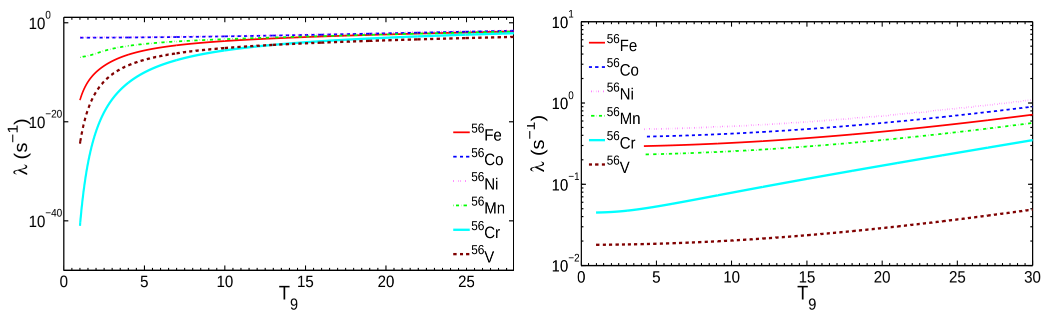

Fig. 2 The EC rates as a function of T_9 at the density $\rho_7 = 5.86, Y_\mathrm{e} = 0.47$ (*left*) and $\rho_7 = 106, Y_\mathrm{e} = 0.43$ (*right*).

by the EC process. Furthermore, the GT transition is dominate in this process. From these figures, one can see that with an increase of the neutrino energy there are different effects on NES in the EC reaction for different nuclides due to a difference in the nuclide's threshold energy and orbital transitions in the EC reaction.

Compared with the NES for these nuclides from three figures, except for ^{56}Co, we find that the NES values for the other five nuclei are very similar. The NES for the five nuclides peak around rather small neutrino energies $2\,m_\mathrm{e}\,c^2 < E_\nu < 15\,m_\mathrm{e}\,c^2$ with a width of $5\,m_\mathrm{e}\,c^2 < \Delta E_\nu < 15\,m_\mathrm{e}\,c^2$. Due to the negative Q_0 values for these nuclei, the EC reaction is blocked and requires many more electrons from the exponentially decreasing tail of the Fermi-Dirac distribution. Thus, the EC to low-lying states occurs in electrons with lower energies than the bulk of the GT strength, but both are accompanied by low-energy neutrinos.

Figures 6, 7 and 8 show the influence on the NES of these nuclides in different energy states by neutrino energies at $\rho_7 = 10.7, Y_\mathrm{e} = 0.45$ and $T_9 = 15$. One can see that the effect on NES is different for most of the nuclei at different energy states. The lower the electron energy state is, the higher the peak value of NES and the larger the influence on NES are. Due to the different energy values in different states for these nuclides, the influences on NES have a different expression at the same astrophysical conditions.

According to our calculations, the peak values of NES are 9.02, 160, 80, 24.01, 0.44 and 1.42 $m_\mathrm{e}\,c^2$ for ^{56}Fe, ^{56}Co, ^{56}Ni, ^{56}Mn, ^{56}Cr and ^{56}V in the ground states, respectively. By contrast, we can see the higher the energy of the excited state is, the lower the peak value is. From Figures 3 to 8, we can see that the Q_0-value allows the EC reaction to occur with all energies for

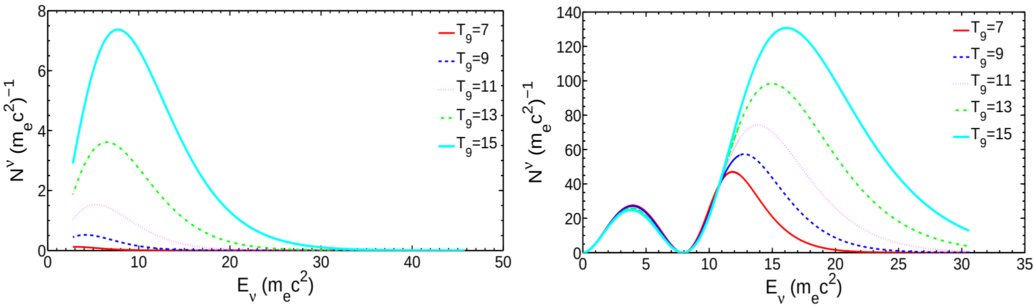

Fig. 3 The NES for ^{56}Fe (*left*) and ^{56}Co (*right*) as a function of the neutrino energy at the density $\rho_7 = 5.86, Y_\mathrm{e} = 0.47$ and temperature of $T_9 = 7, 9, 11, 13$ and 15.

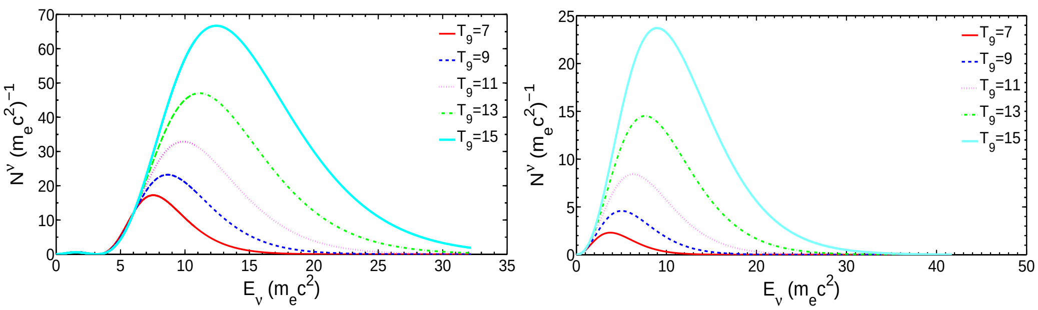

Fig. 4 Same as Fig. 3, but for ^{56}Ni (*left*) and ^{56}Mn (*right*).

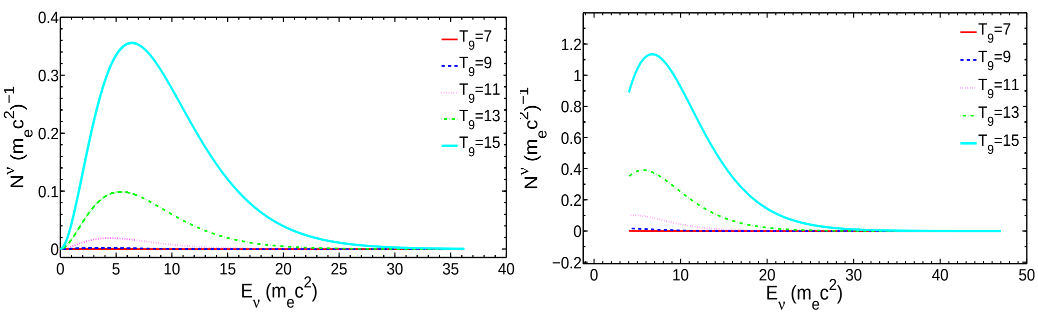

Fig. 5 Same as Fig. 3, but for ^{56}Cr (*left*) and ^{56}V (*right*).

^{56}Ni. However, the GT distribution in the daughter ^{56}Co is concentrated at low excitation energies, resulting again in a different neutrino spectrum. The NES in the EC reaction for ^{56}Mn, ^{56}Cr and ^{56}V does not produce a double-bump structure due to the negative Q_0-value which favors emission of low-energy neutrinos because of the similarity in nuclear structure. However, we find the spectrum of ^{56}Co shows a double bump structure. This is caused by the positive threshold energy Q_0 in the EC process and the partial NES contributed by selected states in the parent nucleus ^{56}Fe.

By analyzing the effect on NES by EC for the different nuclides, we find that the density and temperature have different effects on NES in the EC process for different nuclides because of the difference in the nuclide's threshold energy and transition orbits in the EC reaction. On the other hand, there are different effects on NES in the EC process for different nuclides owing to the difference in the nuclide's ground state and energy of different excited states.

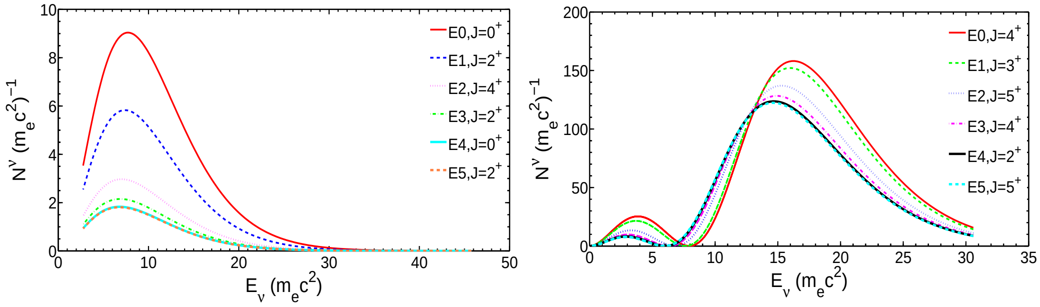

Fig. 6 The NES for ^{56}Fe (*left*) and ^{56}Co (*right*) as a function of the neutrino energy at the ground state and different excited states and the density $\rho_7 = 10.7, Y_{\rm e} = 0.45$ and $T_9 = 15$.

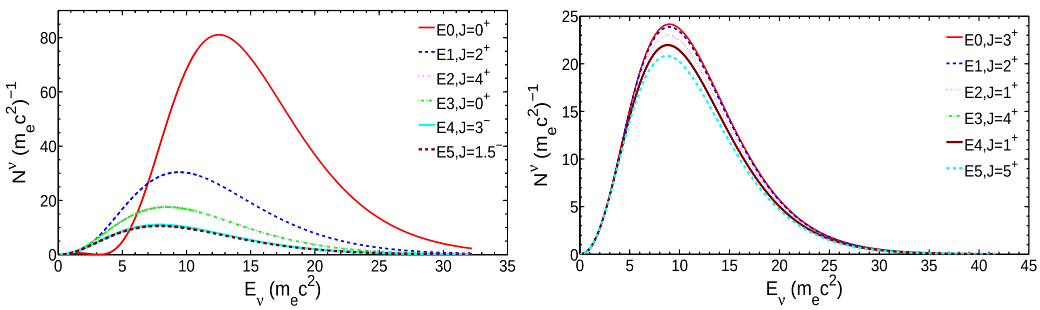

Fig. 7 Same as Fig. 6, but for ^{56}Ni (*left*) and ^{56}Mn (*right*).

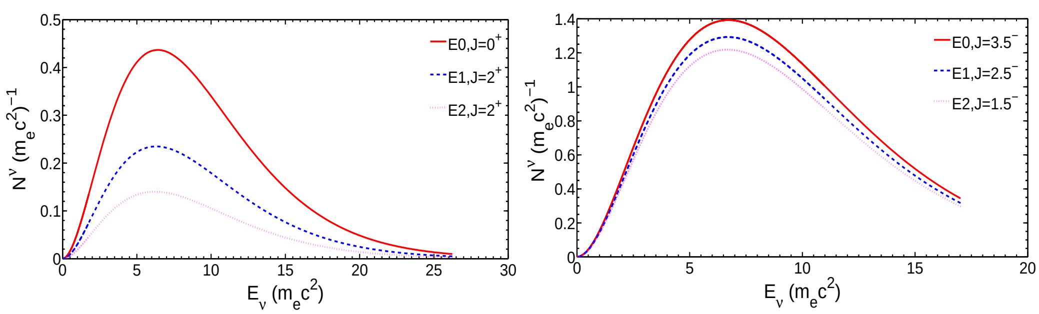

Fig. 8 Same as Fig. 6, but for ^{56}Cr (*left*) and ^{56}V (*right*).

4 CONCLUDING REMARK

Based on the SMMC method and RPA theory, we have carried out an estimation for the NES and EC process of ^{56}Fe, ^{56}Co, ^{56}Ni, ^{56}Mn, ^{56}Cr and ^{56}V in presupernova conditions. The results show that the EC rates are greatly affected at different densities and temperatures. The rates greatly increase and even exceed six orders of magnitude at lower temperature. On one hand, the NES is very sensitive to the stellar temperature and electron energy of different states at different neutrino energy ranges. The higher the temperature and the lower the electron energy are, the larger the influence on NES is. For example, in the ground state, the peak value of NES is 9.02, 160, 80, 24.01, 0.44 and 1.42 $m_{\rm e}\,c^2$ for ^{56}Fe, ^{56}Co, ^{56}Ni, ^{56}Mn, ^{56}Cr and ^{56}V respectively at $\rho_7 = 10.7, Y_{\rm e} = 0.45$

and $T_9 = 15$. On the other hand, the NES for different nuclei shows some otherness because of the different Q_0-values. For example, NES of ^{56}Co shows a double bump structure.

As is well known, in the process of collapse and explosion in a massive star the NES is quite relevant and sensitive in simulations at every point in time and value for density and temperature in the stellar core. The neutrinos are mainly produced by EC and they play a key role. The emerging energy spectra are an important ingredient in the simulations. Due to the escape of a great number of neutrinos by the EC reaction, the NEL contributes one of the key aspects to research about the cooling mechanism in the process of stellar evolution. The NEL is also is very helpful for facilitating the collapse and the explosion of the supernova. Thus, the above conclusions can influence further research in nuclear astrophysics, especially related to the study of cooling systems in the late evolution of massive stars and in simulations of collapse and explosion.

Acknowledgements This work is supported by the Natural Science Foundation of Hainan province (Grant No. 114012).

References

Aufderheide, M. B., Brown, G. E., Kuo, T. T. S., Stout, D. B., & Vogel, P. 1990, ApJ, 362, 241
Aufderheide, M. B., Fushiki, I., Woosley, S. E., & Hartmann, D. H. 1994, ApJS, 91, 389
Cooperstein, J., & Wambach, J. 1984, Nuclear Physics A, 420, 591
Dean, D. J., Langanke, K., Chatterjee, L., Radha, P. B., & Strayer, M. R. 1998, Phys. Rev. C, 58, 536
Fuller, G. M., Fowler, W. A., & Newman, M. J. 1982, ApJS, 48, 279
Holmes, J. A., Woosley, S. E., Fowler, W. A., & Zimmerman, B. A. 1976, Atomic Data and Nuclear Data Tables, 18, 305
Juodagalvis, A., Langanke, K., Hix, W. R., Martínez-Pinedo, G., & Sampaio, J. M. 2010, Nuclear Physics A, 848, 454
Langanke, K., & Martinez-Pinedo, G. 1998, Physics Letters B, 436, 19
Liu, J.-J., Luo, Z.-Q., Liu, H.-L., & Lai, X.-J. 2007a, International Journal of Modern Physics A, 22, 3305
Liu, J.-J., Luo, Z.-Q., Liu, H.-L., & Lai, X.-J. 2007b, Chinese Physics, 16, 2671
Liu, J.-J., & Luo, Z.-Q. 2007a, Chinese Physics Letters, 24, 1861
Liu, J.-J., & Luo, Z.-Q. 2007b, Chinese Physics, 16, 3624
Liu, J.-J., & Luo, Z.-Q. 2008a, Chinese Physics C, 32, 617
Liu, J.-J., & Luo, Z.-Q. 2008b, Chinese Physics C, 32, 108
Liu, J.-J., & Luo, Z.-Q. 2008c, Communications in Theoretical Physics, 49, 239
Liu, J.-J. 2010a, Chinese Physics C, 34, 171
Liu, J.-J. 2010b, Chinese Physics C, 34, 1700
Liu, J.-J., Kang, X.-P., He, Z., et al. 2011, Chinese Physics C, 35, 243
Liu, J.-J. 2012, Chinese Physics Letters, 29, 122301
Liu, J.-J. 2013a, Ap&SS, 343, 117
Liu, J.-J. 2013b, Ap&SS, 343, 579
Liu, J.-J. 2013c, RAA (Research in Astronomy and Astrophysics), 13, 99
Liu, J.-J. 2013d, MNRAS, 433, 1108
Liu, J.-J. 2013e, RAA (Research in Astronomy and Astrophysics), 13, 945
Liu, J.-J. 2013f, Chinese Physics C, 37, 085101
Thielemann, F.-K., Truran, J. W., & Arnould, M. 1986, in Proceedings of the Second IAP Workshop, Advances in Nuclear Astrophysics, eds. E. Vangioni-Flam, J. Audouze, M. Casse, J.-P. Chieze, & J. Tran Thanh Van, 525